Measurement of the ratio $\Gamma(K_L \to \gamma\gamma)/\Gamma(K_L \to \pi^0\pi^0\pi^0)$ with the KLOE detector

The KLOE Collaboration

M. Adinolfi [i], A. Aloisio [e], F. Ambrosino [e], A. Antonelli [b], M. Antonelli [b], C. Bacci [j], G. Bencivenni [b], S. Bertolucci [b], C. Bini [h] C. Bloise [b], V. Bocci [h], F. Bossi [b], P. Branchini [j], S. A. Bulychjov [o], G. Cabibbo [h], R. Caloi [h], P. Campana [b], G. Capon [b], T. Capussela [e], G. Carboni [i], M. Casarsa [ℓ], V. Casavola [d], G. Cataldi [d], F. Ceradini [j], F. Cervelli [f], F. Cevenini [e], G. Chiefari [e], P. Ciambrone [b], S. Conetti [m], E. De Lucia [h], P. De Simone [b], G. De Zorzi [h], S. Dell'Agnello [b], A. Denig [c], A. Di Domenico [h], C. Di Donato [e], S. Di Falco [f], B. Di Micco [j], A. Doria [e], M. Dreucci [b], O. Erriquez [a], A. Farilla [j], G. Felici [b], A. Ferrari [j], M. L. Ferrer [b], G. Finocchiaro [b], C. Forti [b], A. Franceschi [b], P. Franzini [h], C. Gatti [h], P. Gauzzi [h], A. Giannasi [f], S. Giovannella [b], E. Gorini [d], E. Graziani [j], M. Incagli [f], W. Kluge [c], V. Kulikov [o], F. Lacava [h], G. Lanfranchi [b 1], J. Lee-Franzini [b,k], D. Leone [h], F. Lu [b,n] M. Martemianov [b], M. Matsyuk [b], W. Mei [b], L. Merola [e], R. Messi [i], S. Miscetti [b], M. Moulson [b], S. Müller [c], F. Murtas [b], M. Napolitano [e], A. Nedosekin [b,o], F. Nguyen [j], M. Palomba [f], L. Pacciani [i], M. Palutan [b], E. Pasqualucci [h], L. Passalacqua [b], A. Passeri [j], V. Patera [b,g], F. Perfetto [e], E. Petrolo [h], G. Pirozzi [e], L. Pontecorvo [h], M. Primavera [d], F. Ruggieri [a], P. Santangelo [b], E. Santovetti [i], G. Saracino [e], R. D. Schamberger [k], B. Sciascia [b], A. Sciubba [b,g], F. Scuri [f], I. Sfiligoi [b], A. Sibidanov [b], T. Spadaro [b], E. Spiriti [j], M. Tabidze [b,p], G. L. Tong [b,n], L. Tortora [j], P. Valente [b], B. Valeriani [c], G. Venanzoni [f], S. Veneziano [h], A. Ventura [d], S.Ventura [h], R.Versaci [j]

[1] Corresponding author: G. Lanfranchi, e-mail Gaia.Lanfranchi@lnf.infn.it

[a] *Dipartimento di Fisica dell'Università e Sezione INFN, Bari, Italy.*

[b] *Laboratori Nazionali di Frascati dell'INFN, Frascati, Italy.*

[c] *Institut für Experimentelle Kernphysik, Universität Karlsruhe, Germany.*

[d] *Dipartimento di Fisica dell'Università e Sezione INFN, Lecce, Italy.*

[e] *Dipartimento di Scienze Fisiche dell'Università "Federico II" e Sezione INFN, Napoli, Italy*

[f] *Dipartimento di Fisica dell'Università e Sezione INFN, Pisa, Italy.*

[g] *Dipartimento di Energetica dell'Università "La Sapienza", Roma, Italy.*

[h] *Dipartimento di Fisica dell'Università "La Sapienza" e Sezione INFN, Roma, Italy.*

[i] *Dipartimento di Fisica dell'Università "Tor Vergata" e Sezione INFN, Roma, Italy.*

[j] *Dipartimento di Fisica dell'Università "Roma Tre" e Sezione INFN, Roma, Italy.*

[k] *Physics Department, State University of New York at Stony Brook, USA.*

[ℓ] *Dipartimento di Fisica dell'Università e Sezione INFN, Trieste, Italy.*

[m] *Physics Department, University of Virginia, USA.*

[n] *Permanent address: Institute of High Energy Physics, CAS, Beijing, China.*

[o] *Permanent address: Institute for Theoretical and Experimental Physics, Moscow, Russia.*

[p] *Permanent address: High Energy Physics Institute, Tbilisi State University, Tbilisi, Georgia.*

Abstract

We have measured the ratio $R = \Gamma(K_L \to \gamma\gamma)/\Gamma(K_L \to \pi^0\pi^0\pi^0)$ using the KLOE detector. From a sample of $\sim 10^9$ ϕ-mesons produced at DAΦNE, the Frascati $\phi-$factory, we select $\sim 1.6\ 10^8$ K_L-mesons tagged by observing $K_S \to \pi^+\pi^-$ following the reaction $e^+e^- \to \phi \to K_L K_S$. From this sample we select 27,375 $K_L \to \gamma\gamma$ events and obtain $R = (2.79 \pm 0.02_{stat} \pm 0.02_{syst}) \times 10^{-3}$. Using the world average value for $BR(K_L \to \pi^0\pi^0\pi^0)$, we obtain $BR(K_L \to \gamma\gamma) = (5.89 \pm 0.07 \pm 0.08) \times 10^{-4}$ where the second error is due to the uncertainty on the $\pi^0\pi^0\pi^0$ branching fraction.

PACS:

keywords:

---

1 Introduction and experimental setup

The decays $K_S \to \gamma\gamma$ and $K_L \to \gamma\gamma$ provide interesting tests [1] of chiral perturbation theory, ChPT. The dominant contribution to the $K_S \to \gamma\gamma$ decay is $\mathcal{O}(p^4)$ and can therefore be computed with reasonable accuracy in ChPT. The $\mathcal{O}(p^4)$ term vanishes for $K_L \to \gamma\gamma$ in the SU(3) limit. However large $\mathcal{O}(p^6)$ contributions mediated by pseudoscalar mesons [2] are expected for $K_L \to \gamma\gamma$ with values depending on the amount of singlet-octet mixing [3]. A precise measurement of the $K_L \to \gamma\gamma$ decay rate is also of interest in connection with the $K_L \to \mu^+\mu^-$ decay. In fact the absorptive part of the decay rate, $\Gamma(K_L \to \mu^+\mu^-)_{abs}$, is proportional to $\Gamma(K_L \to \gamma\gamma)$. This constrains the dispersive part, $\Gamma(K_L \to \mu^+\mu^-)_{dis}$ and eventually the possibility of determining the V_{td} parameter of the CKM matrix [1]. Measurements of $\Gamma(K_S \to \gamma\gamma)/\Gamma(K_S \to \pi^0\pi^0)$ and $\Gamma(K_L \to \gamma\gamma)/\Gamma(K_L \to \pi^0\pi^0\pi^0)$ have been recently published by the NA48 Collaboration [4]. We describe a new measurement of $\Gamma(K_L \to \gamma\gamma)/\Gamma(K_L \to \pi^0\pi^0\pi^0)$ obtained with K_L-mesons from $\phi \to K_S K_L$ decays at DAΦNE, the Frascati $\phi-$factory.

In DAΦNE the electron and positron beams have energy $E = m_\phi/(2\cos\theta)$ where $\theta = 12.5$ mrad is half of the beam crossing angle. ϕ-mesons are produced with a cross section of ~ 3 μb and a momentum of 12.5 MeV/c toward the center of the rings.

The center of mass energy, W, the position of the beam crossing point (x, y, z) and the ϕ momentum are determined by measuring Bhabha scattering events. In a typical run of integrated luminosity $\int \mathcal{L}\mathrm{dt} \sim 100$ nb^{-1}, lasting about 30 minutes, we have $\delta W = 40$ keV, $\delta p_\phi = 30$ keV/c, $\delta x = 30$ μm, and $\delta y = 30$ μm.

The detector consists of a large cylindrical drift chamber, DC [6], surrounded by a lead-scintillating fiber sampling calorimeter, EMC [7], both immersed in a solenoidal magnetic field of 0.52 T with the axis parallel to the beams. The DC tracking volume extends from 28.5 to 190.5 cm in radius and is 340 cm in length. For charged particles the transverse momentum resolution is $\delta p_T/p_T \simeq 0.4\%$ and vertices are reconstructed with a spatial resolution of $\sim$ 3 mm. The calorimeter is divided into a barrel and two endcaps and covers 98% of the solid angle. Photon energies and arrival times are measured with resolutions $\sigma_E/E = 0.057/\sqrt{E\ (\mathrm{GeV})}$ and $\sigma_t = 54\ \mathrm{ps}/\sqrt{E\ (\mathrm{GeV})} \oplus 50$ ps respectively. The photon entry points are determined with an accuracy $\sigma_l \sim 1\ \mathrm{cm}/\sqrt{E\ (\mathrm{GeV})}$ along the fibers, and ~ 1 cm in the transverse directions. A photon is defined as a calorimeter cluster not associated to a charged particle, by requiring that the distance along the fibers between the cluster centroid and the impact point of the nearest extrapolated track be greater than $3\sigma_l$. Two small calorimeters, QCAL [8], made with lead and scintillating tiles are wrapped around the low-beta quadrupoles to complete the hermeticity.

The trigger [9] uses information from both the calorimeter and the drift chamber. The EMC trigger requires two local energy deposits above threshold ($E > 50$ MeV in the barrel, $E > 150$ MeV in the endcaps). Recognition and rejection of cosmic-ray events is also performed at the trigger level, checking for the presence of two energy deposits above 30 MeV in the outermost calorimeter plane. The DC trigger is based on the multiplicity and topology of the hits in the drift cells. The trigger has a large time spread with respect to the beam crossing time. It is however synchronized with the machine radio frequency divided by four, $T_{\rm sync} = 10.85$ ns, with an accuracy of 50 ps. During the period of data taking the bunch crossing period at DAΦNE was $T = 5.43$ ns. The T_0 of the bunch crossing producing an event is determined offline during the event reconstruction.

2 Data analysis

The ϕ-meson decays into $K_S K_L \sim 34\%$ of the time. The production of a K_L is tagged by the observation of a $K_S \to \pi^+\pi^-$ decay. $K_L \to \gamma\gamma$ and $K_L \to \pi^0\pi^0\pi^0$ decay vertices are reconstructed along the direction opposite to the K_S in the ϕ rest frame and required to be inside a given fiducial volume, FV. We call $R = N_{\gamma\gamma}/N_{\pi^0\pi^0\pi^0}$ the ratio of interest. The numerators and denominators are found from:

$$N = \frac{N_{obs} - N_{bgd}}{\epsilon_{trig} \cdot \epsilon_{tag} \cdot \epsilon_{FV} \cdot \epsilon_{sel}}$$

where N_{obs} and N_{bgd} are the numbers of observed events and estimated background, ϵ_{trig}, ϵ_{tag}, ϵ_{FV} and ϵ_{sel} are respectively the trigger efficiency, the tagging efficiency, the acceptance in the fiducial volume and the selection efficiency for the two decays. The efficiencies ϵ_{tag} and ϵ_{trig} are equal at the few per mil level and cancel in the ratio R. Background and selection efficiencies must be separately determined.

For this analysis the drift chamber is used to measure the $K_S \to \pi^+\pi^-$ decay and to determine the direction of the K_L, the calorimeter is used to measure the photon energies and impact points and to reconstruct the K_L decay vertex by time of flight.

The data sample was collected during 2001 and 2002 for an integrated luminosity of ~ 362 pb^{-1} corresponding to the production of $\sim 10^9$ ϕ. Details of the analysis can be found in reference [10]. $K_L \to \gamma\gamma$ events have a very clear signature, being the only source of ~ 250 MeV photon pairs that balance the momentum of the observed K_S. This allows the use of very loose selection criteria. On the other hand $K_L \to \pi^0\pi^0\pi^0$, the dominant neutral decay, is

characterised by a large multiplicity of lower energy photons. The final error on R is dominated by the error on the number of $K_L \to \gamma\gamma$ events.

Before full event reconstruction, the data are passed through a filter to reject machine background and cosmic ray events. As discussed later, this filter has a modest impact on the events of interest for this analysis.

$K_S \to \pi^+\pi^-$ decays are selected with the following requirements:

- two tracks with opposite charge that form a vertex with cylindrical coordinates $r_v < 4$ cm, $|z_v| < 8$ cm, and no other tracks connected to the vertex;
- K_S momentum 100 MeV/c $< p_{\vec{K_S}} = \vec{p}_{\pi^+} + \vec{p}_{\pi^-} <$ 120 MeV in the ϕ rest system, and $\pi^+\pi^-$ invariant mass 490 MeV $< M_{\pi^+\pi^-} <$ 505 MeV.

The $K_S \to \pi^+\pi^-$ decay provides an unbiased tag for the K_L when it decays into neutral particles and a good measurement of the K_L momentum, $\vec{p}_{K_L} = \vec{p}_\phi - \vec{p}_{K_S}$, where $\vec{p}_\phi$ is the central value of the e^+e^- momentum determined with Bhabha scattering events. The angular resolution on the K_L direction is determined from $K_L \to \pi^+\pi^-\pi^0$ events by measuring the angle between $\hat{p}_{K_L}$ and the line joining the ϕ vertex and the $\pi^+\pi^-$ reconstructed vertex. The widths of the angular distributions are $\delta\phi = 1.5°$, $\delta\theta = 1.8°$.

The position of the K_L vertex for $K_L \to \gamma\gamma$ and $K_L \to \pi^0\pi^0\pi^0$ decays is measured using the photon arrival times on the EMC. Each photon defines a time of flight triangle shown in Fig. 1. The three sides are the K_L decay length, L_K; the distance from the decay vertex to the calorimeter cluster centroid, L_γ; and the distance from the cluster to the ϕ vertex, L. The equations to determine the unknowns L_K and L_γ are:

$$\begin{aligned} L^2 + L_K^2 - 2LL_K\cos\theta &= L_\gamma^2 \\ L_K/\beta_K + L_\gamma &= ct_\gamma \end{aligned}$$

where t_γ is the photon arrival time on the EMC, $\beta_K c$ is the K_L velocity and θ is the angle between $\vec{L}$ and $\vec{L}_K$. Only one of the two solutions is kinematically correct. The value of L_K is obtained from the energy weighted average, $L_K = \sum_i E_i \cdot L_{Ki} / \sum_i E_i$ where i is the photon index.

The accuracy of this method is checked by comparing in the $K_L \to \pi^+\pi^-\pi^0$ decays the position of the K_L decay vertex measured both by timing with the calorimeter and, with a much better precision, by tracking with the drift chamber.

The resolution function, $\sigma(L_K)$, is determined with $K_L \to \pi^0\pi^0\pi^0$ and $K_L \to \gamma\gamma$ events by the distribution of the residuals $L_{K,i} - L_K$ where L_K is the average

obtained with all the photons but the i^{th}. We measure for the $K_L \to \pi^0\pi^0\pi^0$ sample $\sigma_{\pi^0\pi^0\pi^0}(L_K) = 2.06 - (0.16 \cdot 10^{-2}\ L_K) + (0.19 \cdot 10^{-4}\ L_K^2)$ (cm) and for the $K_L \to \gamma\gamma$ sample $\sigma_{\gamma\gamma}(L_K) = 1.73 + 0.0033\ L_K$ (cm).

The K_L FV is defined in cylindrical coordinates as 30 cm $< r_t <$ 170 cm, $|z| <$ 140 cm. The fraction of K_L-mesons decaying in the FV is $(31.5 \pm 0.1)\%$.

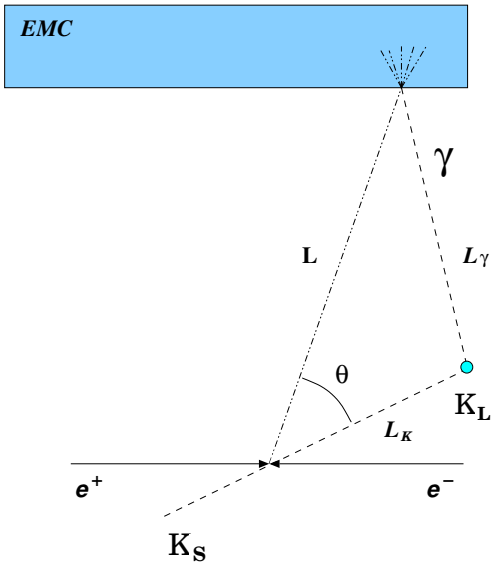

Fig. 1. The time of flight triangle

The identification of the bunch crossing that originated the event is crucial to locate the vertex in space. An error by one bunch crossing period results in a displacement of the K_L vertex of about 33 cm and decreases the probability of correctly associating the photon clusters. The bunch crossing is determined by identifying one of the two pions of the K_S decay and by measuring its track length, momentum and time of flight. Thus an error of one (or more) crossing periods can occur if there is an incorrect track-to-cluster association or the track parameters are poorly measured.

To minimise the number of events with an incorrect bunch-crossing assignment, we perform a consistency check of the time of flight of the pions along their trajectory l_π measured with the DC, $t_{DC} = l_\pi/\beta_\pi\gamma_\pi c$ with the corresponding cluster time measured by the calorimeter, t_{EMC}. Requiring $|t_{DC} - t_{EMC}| < 2$ ns for at least one pion, the probability of correctly identifying the bunch crossing is $(99.4 \pm 0.1)\%$. This additional cut retains 96% of the original $K_S \to \pi^+\pi^-$ event sample. The probability of identifying the correct bunch crossing was measured with a sample of $K_L \to \pi^+\pi^-\pi^0$ decays where the position of the $\pi^+\pi^-$ vertex, $r_{\pi\pi}$, is reconstructed by tracking in the DC and the position of the two-photon vertex, $r_{\gamma\gamma}$, by timing with the EMC. The difference $r_{\pi\pi} - r_{\gamma\gamma}$ is used to isolate the events in which the bunch crossing is incorrectly determined.

3 $K_L \to \pi^0\pi^0\pi^0$ selection

The $K_L \to \pi^0\pi^0\pi^0$ decay has a large branching fraction, 21%, and thus has very small background. Given the large statistics we retain only 1 out of 10 decays. The selection of $K_L \to \pi^0\pi^0\pi^0$ events requires at least three calorimeter clusters with the following properties

- energy larger than 20 MeV;
- distance from any other cluster larger than 40 cm;
- no association to a charged track;
- L_K in the fiducial volume and $|L_{Ki} - L_K| < 4\sigma(L_K)$.

The main sources of inefficiencies are: 1) geometrical acceptance; 2) cluster energy threshold; 3) merging of clusters; 4) accidental association to a charged track; 5) Dalitz decay of one or more π^0's. The effect of these inefficiencies is to modify the relative population for events with 3, 4, 5, 6, 7 and ≥ 8, clusters without significant loss of efficiency. Monte Carlo simulation shows that the selection efficiency is $\epsilon_{sel} = (99.80 \pm 0.01)\%$.

A comparison between data and Monte Carlo of the relative populations and of the distribution of the total energy, $E = \sum_i E_i$, shows that only events with 3 and 4 clusters are contaminated by background. This is due to $K_L \to \pi^+\pi^-\pi^0$ decays where one or two charged pions produce a cluster not associated to a track and neither track is associated to the K_L vertex or to $K_L \to \pi^0\pi^0$ decays, possibly in coincidence with machine background particles ($e^\pm$ or γ) that shower in the QCAL and generate soft neutral particles.

To reduce this background, for the 3-cluster population we further require at least two clusters in the barrel with at least one of them with energy $E > 50$ MeV and for the 4-cluster population at least one cluster in the barrel with energy $E > 50$ MeV. The probability to have a cluster with $E > 50$ MeV has been evaluated using the 6-cluster events. The probability of having a given number of clusters in the barrel depends only on geometry and has been evaluated by Monte Carlo simulation. We obtain $\epsilon_{3,E>50\mathrm{MeV}} = (81.9 \pm 0.1)\%$ and $\epsilon_{4,E>50\mathrm{MeV}} = (98.3 \pm 0.1)\%$. Additionally, an event with 3 clusters is accepted only if an additional cluster is found in QCAL within a time window of 10 ns with respect to the K_L decay time. The probability of such an occurrence is $\epsilon_{qcal} = (52 \pm 2)\%$.

The $K_L \to \pi^+\pi^-\pi^0$ background is rejected by imposing a veto (*track veto*) on the events with charged tracks not associated to the K_S decay and with the first hit in the drift chamber at a distance of less than 30 cm from the position of the K_L vertex. The track veto also rejects about 60% of the $K_L \to \pi^0\pi^0\pi^0$ events with Dalitz decays.

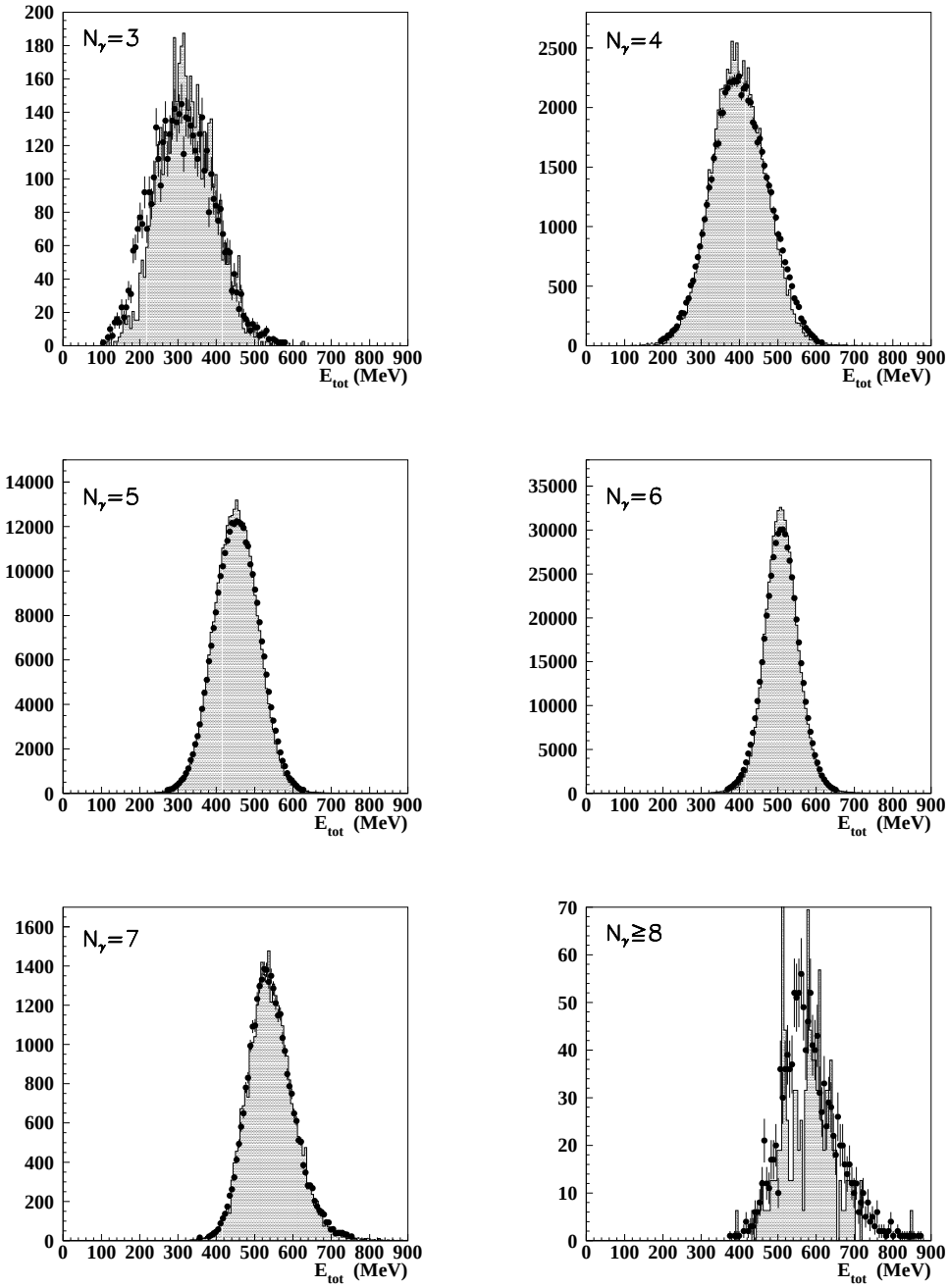

Fig. 2. $K_L \to \pi^0\pi^0\pi^0$ selection: distribution of the total energy for events with 3, 4, 5, 6, 7 and ≥ 8 clusters. Dots are data, shaded histogram is Monte Carlo simulation for $K_L \to$ all channels. Data and Monte Carlo histograms are normalized to the same number of entries.

Fig. 2 shows the distribution of the total energy for events with different numbers of clusters together with the results of the Monte Carlo simulation. The relative fraction of events is shown in Table 1. The difference between data and Monte Carlo simulation for events with ≥ 5 clusters is due to split clusters.

The contamination from accidental clusters originated by machine background is negligible. The residual background contamination in events with 3 and 4 clusters is evaluated by Monte Carlo simulation and amounts to $(18.6 \pm 1.0)\%$ and $(7.0 \pm 0.2)\%$ respectively.

Number of clusters	Data	Monte Carlo
3	0.37 ± 0.02 %	0.35 ± 0.04 %
4	7.2 ± 0.1 %	7.3 ± 0.1 %
5	31.5 ± 0.1 %	32.2 ± 0.2 %
6	57.4 ± 0.1 %	58.4 ± 0.2 %
7	3.3 ± 0.1 %	1.7 ± 0.1 %
≥ 8	0.1 %	0.03 %

Table 1
Fraction of events with at least three neutral clusters connected to the K_L decay vertex.

A subsample of events has been processed and analysed without passing through the initial filter. The fractional loss due to the filter is found to be less than 10^{-3}. The trigger efficiency for $K_S \to \pi^+\pi^-, K_L \to \pi^0\pi^0\pi^0$ events was measured in two different ways. A detailed description of the methods is given in reference [9]. The first method uses only the data and the information provided by the combined EMC + DC trigger. In the second method the Monte Carlo is used to evaluate the correlation between the EMC and the DC trigger showing that the correlation factor is very small. The results obtained with the two methods, $\epsilon_{trig1} = (99.88 \pm 0.04)\%$, $\epsilon_{trig2} = (99.90 \pm 0.03)\%$, are in good agreement. Since the two methods are independent, and the results consistent, we combined the two results.

The number of events is:

$$N_{\pi^0\pi^0\pi^0} = \frac{N_3' + N_4' + N_5 + N_6 + N_7 + N_{\geq 8} + N_{Dalitz}}{\epsilon_{downscale} \cdot \epsilon_{trig} \cdot \epsilon_{sel}}$$

where N_3' and N_4' are corrected for the background subtraction and the additional cuts quoted before. N_{Dalitz}, a small addition of 0.46% of the total count, is obtained using the Monte Carlo result that 21.5% of the Dalitz decays are included in $N_3 + N_4$ events while 60% of them are rejected by the track veto. We find $N_{\pi^0\pi^0\pi^0} = 9,802,200 \times \ (1 \pm 0.0010_{stat} \pm 0.0016_{syst})$.

To check the uniformity of the $K_L \to \pi^0\pi^0\pi^0$ vertex reconstruction efficiency throughout the FV we have studied the proper time distribution. From a fit to the distribution we find $\tau_{K_L} = 51.6$ ns with a statistical error of 0.4 ns [10], in good agreement with the value reported in PDG [5], $\tau_{K_L} = (51.7 \pm 0.4)$ ns.

4 $K_L \to \gamma\gamma$ selection

$K_L \to \gamma\gamma$ events are preselected by requiring at least two calorimeter clusters with energy $E_\gamma > 100$ MeV not associated to tracks. For the two most energetic clusters we require:

- total energy, $E_{12} = E_{\gamma 1} + E_{\gamma 2} > 350$ MeV;
- angle between the photon momenta projected onto the plane normal to the K_L direction, $\psi > 150°$;
- time difference smaller than 15 ns;
- K_L decay vertex in the fiducial volume and $\Delta L_K = |L_{K1} - L_{K2}| < 4\sigma_{\gamma\gamma}(L_K)$.

The geometrical acceptance and the selection efficiency are evaluated by Monte Carlo simulation. The values of the efficiency are shown in table 2.

preselection	efficiency
$E_\gamma > 100$ MeV)	$(92.6 \pm 0.1_{stat})$ %
$E_{12} > 350$ MeV	$(99.88 \pm 0.02_{stat})$ %
$\psi > 150°$	$(98.4 \pm 0.1_{stat} \pm 0.4_{syst})$ %
$\Delta L_K < 4\sigma$	$(98.5 \pm 0.1_{stat} \pm 0.2_{syst})$ %
$\Delta t < 15$ ns	$(99.89 \pm 0.02_{stat})$ %
total	$(89.5 \pm 0.2_{stat} \pm 0.4_{syst})$ %

Table 2
Efficiency of the $K_L \to \gamma\gamma$ preselection.

With these cuts we obtain 1.7×10^5 events with a large background due to $K_L \to \pi^0\pi^0\pi^0$ and $K_L \to \pi^0\pi^0$ decays, $K_L \to \gamma\gamma\gamma$ being negligible [11].

The signal is further selected using the two body $K_L \to \gamma\gamma$ decay kinematics. In fact, photon energies can be computed with better accuracy from cluster and decay vertex coordinates. The laboratory energy is obtained by boosting from the center of mass where $E_\gamma = M_K/2$ to the laboratory. If $\hat{p}_{\gamma i}$ are unit vectors from the K_L decay vertex to the cluster centroids, the photon energies are

$$E'_{\gamma i} = \frac{M_K/2}{\gamma_K(1 - \beta_K\ \hat{p}_{\gamma i} \cdot \hat{p}_K)}$$

where β_K and $\hat{p}_K$ are computed from $\vec{p}_{K_L} = \vec{p}_\phi - \vec{p}_{K_S}$. The K_L has energy $E' = E'_{\gamma 1} + E'_{\gamma 2}$, and momentum $\vec{p}_{\gamma\gamma} = E'_{\gamma 1} \cdot \hat{p}_{\gamma 1} + E'_{\gamma 2} \cdot \hat{p}_{\gamma 2}$. Fig. 3 shows the distribution of E' and of the angle α between $\vec{p}_{\gamma\gamma}$ and $\vec{p}_{K_L}$, together with the results of the Monte Carlo simulation. The data are fitted with a linear

combination of the Monte Carlo distributions for signal and background. The fit gives the relative normalisation for the two populations.

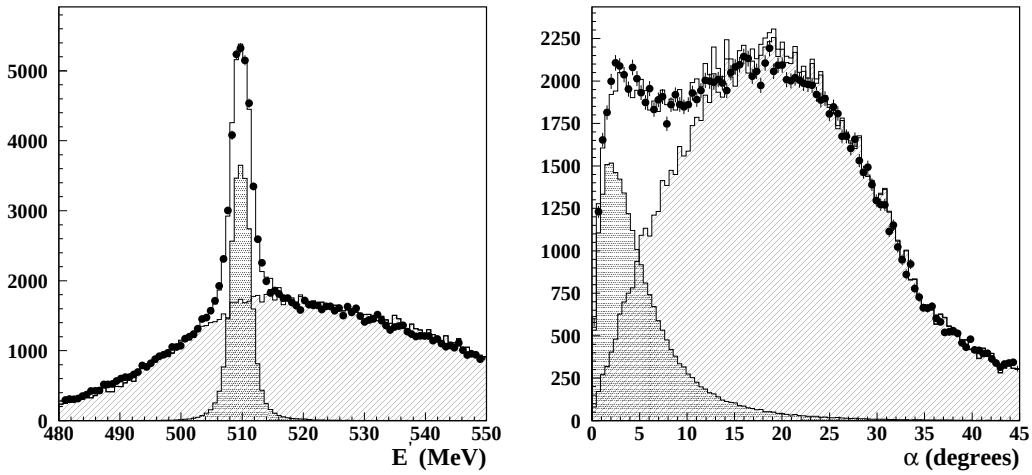

Fig. 3. $K_L \to \gamma\gamma$ selection: distributions of laboratory total energy E' (left) and the angle α between $\vec{p}_{\gamma\gamma}$ and $\vec{p}_{K_L}$ (right). Dots are data, shaded histogram is Monte Carlo simulation for the signal, dashed histogram is Monte Carlo simulation for background and solid line histogram is the Monte Carlo simulation for signal and background.

In order to reduce background we further require:

- $|E' - \mu'| < 5\sigma'$ where $\mu' = 510.0$ MeV and $\sigma' = 1.8$ MeV are evaluated from a fit to the E' distribution;
- $\alpha < 15^\circ$.

To extract the signal we fit the invariant mass $M_{\gamma\gamma}$ distribution obtained using calorimeter cluster energies with a linear combination of the Monte Carlo distributions for signal and background. The result of the fit gives the number of events for the two populations. Fig. 4 shows the distribution of $M_{\gamma\gamma}$ before and after the E' and α cuts. From a fit to the second distribution we find $22,185 \pm 170$ $K_L \to \gamma\gamma$ events.

The efficiency of the selection cuts are evaluated from the data using a sample of $K_L \to \gamma\gamma$ events with high purity (S/B $\sim 10^3$) selected by applying hard, uncorrelated cuts on other kinematic variables [10].

The systematic error associated with the selection cuts on (E', α) is evaluated by moving the cuts around the chosen values and fitting the invariant mass distribution. The maximum displacement of the measured value for the number of signal counts is $\pm 0.2\%$ and $\pm 0.3\%$ for the E' and the α distribution respectively. The systematic error due to the background contamination has been evaluated by changing the shape of the background distribution used as

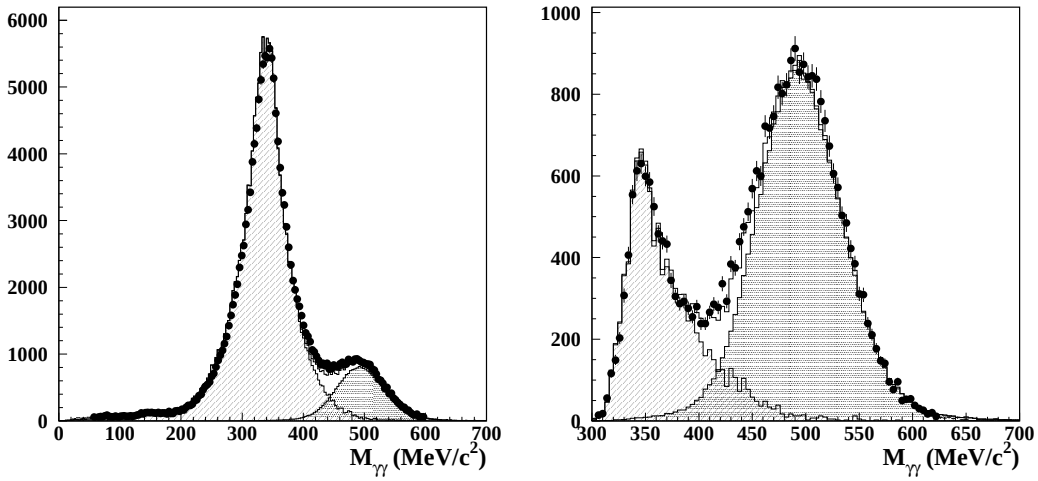

Fig. 4. $K_L \to \gamma\gamma$ selection: distributions of the invariant mass, $M_{\gamma\gamma}$, before (left) and after (right) the E' and α cuts. Dots are data, shaded histogram is Monte Carlo simulation for the signal, dashed histogram is Monte Carlo simulation for background and solid line is the Monte Carlo simulation for signal and background.

input of the fit. The effect on the signal is 10 times smaller and produces a systematic error of $\pm 0.3\%$.

The filter and the trigger efficiencies are evaluated as for the analysis of $K_L \to \pi^0\pi^0\pi^0$ decay. The results are $\epsilon_{filter} = (99.93 \pm 0.01)\%$, $\epsilon_{trig} = (99.44 \pm 0.04)\%$ where the statistical and systematic errors are combined in quadrature. The efficiencies associated with the various analysis steps are summarised in Table 3.

selection	efficiency
trigger	(99.44 ± 0.04) %
filter	(99.93 ± 0.01) %
preselection	$(89.5 \pm 0.2_{stat} \pm 0.4_{syst})$ %
$\lvert E' - \mu' \rvert < 5\sigma'$	$(98.5 \pm 0.2_{stat} \pm 0.2_{syst})$ %
$\alpha < 15^\circ$	$(92.5 \pm 0.3_{stat} \pm 0.3_{syst})$ %
total	$(81.0 \pm 0.3_{stat} \pm 0.5_{syst})$ %

Table 3
Efficiencies for the selection of $K_L \to \gamma\gamma$ events.

The number of events is $N_{\gamma\gamma} = 27,375 \times\ (1 \pm 0.0076_{stat} \pm 0.0081_{syst})$. For the ratio we find:

$$R = \frac{\Gamma(K_L \to \gamma\gamma)}{\Gamma(K_L \to \pi^0\pi^0\pi^0)} = (2.793 \pm 0.022_{stat} \pm 0.024_{syst}) \times 10^{-3}$$

in good agreement with the recent result from the NA48 Collaboration $\Gamma(K_L \to \gamma\gamma)/\Gamma(K_L \to \pi^0\pi^0\pi^0) = (2.81 \pm 0.01_{stat} \pm 0.02_{syst}) \times 10^{-3}$ [4].

Using the known value for the $K_L \to \pi^0\pi^0\pi^0$ branching fraction, we obtain $BR(K_L \to \gamma\gamma) = (5.89 \pm 0.07 \pm 0.08) \times 10^{-4}$ where the first error represents the statistical and systematic error on R combined in quadrature and the second is due to the uncertainty in the $\pi^0\pi^0\pi^0$ branching fraction. A decay width of $\Gamma(K_L \to \gamma\gamma) = (7.5 \pm 0.1) \times 10^{-12}$ eV is in agreement with $\mathcal{O}(p^6)$ predictions of ChPT provided the value of the pseudoscalar mixing angle is close to our recent measurement of $\theta_P = (-12.9^{+1.9}_{-1.6})^\circ$ [12].

Acknowledgements

We thank the DAFNE team for their efforts in maintaining low background running conditions and their collaboration during all data-taking.

We want to thank our technical staff: G.F.Fortugno for his dedicated work to ensure an efficient operation of the KLOE Computing Center; M.Anelli for his continuous support to the gas system and the safety of the detector; A.Balla, M.Gatta, G.Corradi and G.Papalino for the maintenance of the electronics; M.Santoni, G.Paoluzzi and R.Rosellini for the general support to the detector; C.Pinto (Bari), C.Pinto (Lecce), C.Piscitelli and A.Rossi for their help during shutdown periods.

This work was supported in part by DOE grant DE-FG-02-97ER41027; by EURODAPHNE, contract FMRX-CT98-0169; by the German Federal Ministry of Education and Research (BMBF) contract 06-KA-957; by Graduiertenkolleg 'H.E. Phys. and Part. Astrophys.' of Deutsche Forschungsgemeinschaft, Contract No. GK 742; by INTAS, contracts 96-624, 99-37; and by TARI, contract HPRI-CT-1999-00088.

References

[1] G. D'Ambrosio, G. Ecker, G. Isidori and H. Neufeld, "Radiative non-leptonic kaon decays", in The Second DAΦNE Physics Handbook, eds. L. Maiani, G. Pancheri and N. Paver, Vol.I, p.265, 1995.

[2] E. Ma and B. R. Holstein, Phys. Rev. D 24 (1984) 2346; J. F. Donoghue, B. R. Holstein and Y-C. R. Lin, Nucl. Phys. B277 (1986) 651.

[3] G. D'Ambrosio and D. Espriu, Phys. Lett. B175 (1986) 237.

[4] A. Lai et al., Phys. Lett. B551 (2003) 7.

[5] K. Hagiwara et al., Phys. Rev. D66 (2002) 010001-1.

[6] The KLOE Collaboration, M. Adinolfi et al., Nucl. Instr. and Meth. A488 (2002) 51.

[7] The KLOE Collaboration, M. Adinolfi et al., Nucl. Instr. and Meth. A482 (2002) 363.

[8] The KLOE Collaboration, M. Adinolfi et al., Nucl. Instr. and Meth. A483 (2002) 649.

[9] The KLOE Collaboration, M. Adinolfi et al., Nucl. Instr. and Meth. A492 (2002) 134.

[10] S. Di Falco, G. Lanfranchi and E. Santovetti, *Measurement of the ratio* $\Gamma(K_L \to \gamma\gamma)/\Gamma(K_L \to \pi^0\pi^0\pi^0)$, KLOE note n 182, January 2003.

[11] G. D. Barr et al., Phys. Lett. B358 (1995) 399.

[12] The KLOE Collaboration, A. Aloisio et al., Phys. Lett. B541 (2002) 45.